Inorg. Chem. **2003**, *42*, 6589–6591

$[CH_3(CH_2)_{11}NH_3]SnI_3$: A Hybrid Semiconductor with MoO_3-type Tin(II) Iodide Layers

Zhengtao Xu and David B. Mitzi*

IBM T. J. Watson Research Center, P.O. Box 218, Yorktown Heights, New York 10598

Received June 20, 2003

The organic–inorganic hybrid $[CH_3(CH_2)_{11}NH_3]SnI_3$ presents a lamellar structure with a Sn–I framework isotypic to that of MoO_3. The SnI_3^- layer consists of edge and corner-sharing SnI_6 octahedra in which one of the six Sn–I bonds is distinctly elongated (e.g., 3.62 Å), indicating lone-pair stereoactivity for the Sn(II) atom. The overall electronic character remains comparable with that of the well-studied SnI_4^{2-}-based perovskite semiconductors, such as $[CH_3(CH_2)_{11}NH_3]_2SnI_4$, with a red-shifted and broadened exciton peak associated with the band gap, apparently due to the increased dimensionality of the Sn–I framework. The title compound offers, aside from the hybrid perovskites, a new type of solution-processable Sn–I network for potential applications in semiconductive devices.

Organic−inorganic hybrid compounds based on layers of anionic tin(II) iodide frameworks and organic ammonium cations have attracted attention partly because of the highly tunable semiconductive properties imparted by the tin(II) iodide framework and because of the rich structural motifs exhibited by these hybrid systems.[1−13] In the most commonly studied systems, the tin(II) iodide frameworks are derived from the prototypical perovskite $ASnI_3$, where A is the cesium(I) or methylammonium cation or a related monocation of comparable size. Depending on the thickness of the inorganic layer, a general formula can be given to this class of hybrid structures: $(RNH_3)_2A_{n-1}Sn_nI_{3n+1}$ ($n = 1, 2, 3...$), where the A cations continue to occupy the interstices within the inorganic layer and the bulkier organic cation RNH_3^+ forms layers alternating with the inorganic component. The potential technological importance of this group of compounds is well illustrated by the $n = 1$ [i.e., $(RNH_3)_2SnI_4$] members (see Supporting Information for a typical crystal structure), which have been spin-coated from organic solvents or melt-processed into semiconductive channels for thin-film field-effect transistors.[14−17] The choice of different organic cations significantly affects the structure of the SnI_4^{2-} layer, giving rise to variations in the Sn−I−Sn bond angles,[15,17,18] the Sn−I bond distances,[18] the connectivity of the SnI_6 octahedral units,[11,19] and even the interactions between the inorganic sheets.[20] The range of bonding configurations provides rather extensive tunability of the electronic properties of this class of materials.

Despite the large number of reported Sn(II)−I hybrids, the corresponding basic structural types of two-dimensional networks are, however, rather limited. Currently, most are based on the perovskite framework, which, besides the above (100)-oriented $(RNH_3)_2A_{n-1}Sn_nI_{3n+1}$ system, can also be cleaved along the [110] or [111] directions to afford different layered structures consisting of corner-sharing metal halide octahedra.[11] Recently, several rather unique Sn(II)−I-based layer frameworks have been reported.[9,10] In the compound $(Me_3PhN)_4(Sn_3I_{10})$, for example, an octahedral SnI_6^{4-} group first shares two of its opposite faces with two neighboring SnI_6^{4-} groups to form a trimeric unit of $Sn_3I_{10}^{4-}$, which then shares four corner iodine atoms with adjacent units to produce an extended layer. Although both the band gap and processability of these compounds as semiconductive materi-

* To whom correspondence should be addressed. E-mail: dmitzi@us.ibm.com.

(1) Weber, D. *Z. Naturforsch.* **1978**, *33b*, 862.
(2) Weber, D. Z. *Naturforsch.* **1979**, *34b*, 939.
(3) Calabrese, J.; Jones, N. L.; Harlow, R. L.; Herron, N.; Thorn, D. L.; Wang, Y. *J. Am. Chem. Soc.* **1991**, *113*, 2328.
(4) Mitzi, D. B.; Feild, C. A.; Harrison, W. T. A.; Guloy, A. M. *Nature* **1994**, *369*, 467.
(5) Papavassiliou, G. C.; Koutselas, I. B.; Terzis, A.; Whangbo, M.-H. *Solid State Commun.* **1994**, *91*, 695.
(6) Mitzi, D. B.; Wang, S.; Feild, C. A.; Chess, C. A.; Guloy, A. M. *Science* **1995**, *267*, 1473.
(7) Mitzi, D. B.; Feild, C. A.; Schlesinger, Z.; Laibowitz, R. B. *J. Solid State Chem.* **1995**, *114*, 159.
(8) Papavassiliou, G. C.; Koutselas, I. B. *Synth. Met.* **1995**, *71*, 1713.
(9) Lode, C.; Krautscheid, H. *Z. Anorg. Allg. Chem.* **2000**, *626*, 326.
(10) Lode, C.; Krautscheid, H. *Z. Anorg. Allg. Chem.* **2001**, *627*, 1454.
(11) Mitzi, D. B. *J. Chem. Soc., Dalton Trans.* **2001**, 1.
(12) Mitzi, D. B. *Prog. Inorg. Chem.* **1999**, *48*, 1.
(13) Papavassiliou, G. C. *Prog. Solid State Chem.* **1997**, *25*, 125.
(14) Kagan, C. R.; Mitzi, D. B.; Dimitrakopoulos, C. D. *Science* **1999**, *286*, 945.
(15) Mitzi, D. B.; Dimitrakopoulos, C. D.; Kosbar, L. L. *Chem. Mater.* **2001**, *13*, 3728.
(16) Mitzi, D. B.; Dimitrakopoulos, C. D.; Rosner, J.; Medeiros, D. R.; Xu, Z.; Noyan, C. *Adv. Mater.* **2002**, *14*, 1772.
(17) Xu, Z.; Mitzi, D. B.; Dimitrakopoulos, C. D.; Maxcy, K. R. *Inorg. Chem.* **2003**, *42*, 2031.
(18) Tang, Z.; Guan, J.; Guloy, A. M. *J. Mater. Chem.* **2001**, *11*, 479.
(19) Guan, J.; Tang, Z.; Guloy, A. M. *Chem. Commun.* **1999**, 1833.
(20) Xu, Z.; Mitzi, D. B.; Medeiros, D. R. *Inorg. Chem.* **2003**, *42*, 1400.

10.1021/ic0347081 CCC: $25.00
Published on Web 09/18/2003

als are not reported, they represent significant advances toward non-perovskite Sn(II)−I layered structures.

In this paper, we report the non-perovskite-based lamellar hybrid $[CH_3(CH_2)_{11}NH_3]SnI_3$ (**1**), which continues to show solution processability as well as electronic properties similar to those of the perovskite system. For a better comparison, we have also studied the hybrid perovskite $[CH_3(CH_2)_{11}NH_3]_2SnI_4$, which contains the same organic cation as **1**. In contrast to the uniformly corner-sharing octahedra in the perovskite systems, the SnI_6 octahedra in **1** exhibit corner sharing as well as edge sharing with its neighbors, forming a two-dimensional framework similar to that of molybdenum trioxide (MoO_3).[21] The Sn−I framework in **1** is thus thicker than the SnI_4^{2-} perovskite sheet, and it demonstrates a wider range of bonding features between the tin(II) and iodine ions. Despite its more complex Sn(II)−I network, compound **1** can also be solution-processed into thin films at ambient temperatures. Optical absorption measurements of thin-film samples indicate a comparable, albeit noticeably reduced electronic band gap in **1**, with respect to $[CH_3(CH_2)_{11}NH_3]_2SnI_4$. The similar band gap and solution processability of **1** are thus likely to retain the usefulness previously established for hybrid perovskites as a semiconductive material.

Crystals of $[CH_3(CH_2)_{11}NH_3]SnI_3$ (**1**) were formed by evaporating an acetonitrile/anisole solution containing tin(II) iodide (SnI_2) and dodecylammonium iodide $[CH_3(CH_2)_{11}NH_3I]$.[22] Optical absorption spectra of thin film samples[23] of **1** feature an exciton peak (613 nm, 2.02 eV) associated with the band gap, which is significantly red-shifted compared to the perovskite analogue $[CH_3(CH_2)_{11}NH_3]_2SnI_4$ (580 nm, 2.14 eV), as shown in Figure 1. Similarly, **1** shows a corresponding band edge markedly shifted to a longer wavelength, compared with $[CH_3(CH_2)_{11}NH_3]_2SnI_4$. Note also

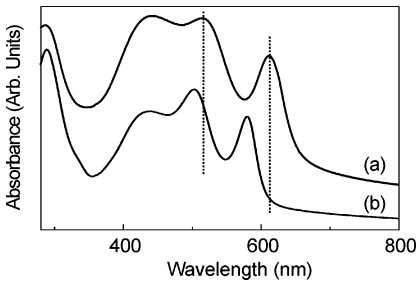

Figure 1. Room-temperature UV−vis absorption spectra for thin films of (a) **1** and (b) $[CH_3(CH_2)_{11}NH_3]_2SnI_4$. The dotted lines highlight the shifts in the peak positions.

that the exciton peak of **1** is broader than that of $[CH_3(CH_2)_{11}NH_3]_2SnI_4$, which presumably reflects the thicker inorganic layer of **1**.[13]

The crystal structure[24] of **1** consists of inorganic layers of the formulae SnI_3^- alternating with organic layers formed by the dodecylammonium cations (Figure 2a). The bonding connectivity of the SnI_3^- framework is similar to that of MoO_3. The basic building units can be considered as the SnI_6 octahedral groups, which share a pair of opposite vertices (i.e., I2 and I5 in Figure 2b) to produce SnI_5 chains along the crystallographic $[1\bar{1}0]$ direction. The individual SnI_5 chains are then merged to furnish the overall SnI_3^- layer by sharing two equatorial edges on each SnI_6 octahedron (Figure 2a,b). Overall, three iodine atoms of each SnI_6 unit are common to three octahedra, two are shared by two, and the sixth is unshared $[(3 \times {}^1/_3) + (2 \times {}^1/_2) + (1 \times 1) = 3]$. The anionic SnI_3^- layers interact with the dodecylammonium layers through the ionic/hydrogen bonding between the iodine atoms and the ammonium groups, with shortest I···N distances between 3.66 and 3.71 Å (I···N van der Waals distance, 3.53 Å[25]). The alkyl chains of the dodecylammonium cations adopt an all-anti conformation and interdigitate, as is also observed in the hybrid perovskites templated by long-chain aliphatic ammonium cations such as $[CH_3(CH_2)_{11}NH_3]_2SnI_4$ (see Supporting Information).[26,27] Such interdigitation provides extensive van der Waals contacts, serving to organize the neighboring inorganic layers into the complete crystal structure.

Distortions of the two crystallographically nonequivalent SnI_6 octahedra exhibit distinct correlation with the bonding environment of the iodine atoms. (1) In either octahedron (Sn1 or Sn2, see Figure 2b), the shortest Sn−I bond is

(21) Wells, A. F. In *Structural Inorganic Chemistry*; Oxford University Press: London, 1962; p 468.

(22) Inside a nitrogen-filled drybox, tin(II) iodide (96 mg, 0.26 mmol) and dodecylammonium iodide (62 mg, 0.20 mmol) were loaded in a vial and mixed with acetonitrile (anhydrous, 6.0 mL). The vial was then capped, and the mixture was stirred at 70 °C for 2 h, after which anisole (anhydrous, 5.0 mL) was added and the residual SnI_2 solid was separated by a Teflon filter (pore size, 0.2 μm) (note that excess SnI_2 was used here to ensure the phase purity of the product, because a strict 1:1 ratio of SnI_2 and dodecylammonium iodide usually yielded a mixture of **1** and the perovskite $[CH_3(CH_2)_{11}NH_3]_2SnI_4$). The transparent yellow filtrate was collected in a vial, and the solvents were allowed to evaporate at room temperature. Platelike, almost black crystals (dark red for thinner crystallites) of **1** were formed over 2 or 3 days. The yield of **1** thus obtained was about 100 mg (73% based on dodecylammonium iodide), although higher yield could likely be achieved with further evaporation of the remaining solution. A powder sample of **1** showed an X-ray diffraction pattern consistent with the single crystal structure (see Supporting Information). Chemical analysis of the product $C_{12}H_{28}NSnI_3$ yielded the following: Calcd [C (21.02%), H (4.12%), N (2.04%)]; Found [C (20.95%), H (4.00%), N (2.16%)].

(23) Thin films were prepared in a N_2-filled drybox by spin-coating a THF/methanol solution on quartz disks. The solution was prepared by dissolving in 0.5 mL of THF and 0.17 mL of methanol 20 mg of a mixture containing dodecylammonium iodide and tin(II) iodide in 1:1.2 molar ratio. Excess SnI_2 is used here to further promote the formation of **1** over $[CH_3(CH_2)_{11}NH_3]_2SnI_4$. The spin cycle is as follows: 1 s to 4000 rpm; dwell 30 s at 4000 rpm. The disk was then heated at 70 °C for 15 min for annealing and solvent removal. The formation of **1** was confirmed by an X-ray scan, although a small peak corresponding to the residual SnI_2 was also observed (see Supporting Information). The film is also highly crystallographically oriented with regard to the disk surface, like hybrid perovskite films {e.g., $[CH_3(CH_2)_{11}NH_3]_2SnI_4$} similarly prepared.

(24) The X-ray data set of **1** was collected at room temperature from a crystal (0.36 × 0.22 × 0.10 mm^3) on a Bruker SMART CCD diffractometer, equipped with a normal focus 2.4 kW sealed tube X-ray source (Mo Kα radiation). The structure was solved by direct methods in $P\bar{1}$ and refined on F^2 (full matrix, absorption corrections with SADABS) using the Shelxl 97 package. Hydrogen atoms were not located from the Fourier map, and all the non-hydrogen atoms were refined anisotropically. Crystal data: triclinic, $P\bar{1}$, $a = 8.8743(7)$ Å, $b = 8.9512(8)$ Å, $c = 26.685(2)$ Å, $\alpha = 84.392(1)°$, $\beta = 85.912(1)°$, $\gamma = 89.491(1)°$, $V = 2104.2(3)$ $Å^3$, $Z = 4$, $\mu = 56.03$ cm^{-1}, $d_{calcd} = 2.165$ g/cm^3, $R_{int} = 2.69\%$, R1/wR2 = 4.66/11.08% for 6249 unique observed reflections [$I \geq 2\sigma(I)$] and 308 variables (R1/wR2 = 7.94/12.60% for all data).

(25) Bondi, A. *J. Phys. Chem.* **1964**, *68*, 441.

(26) Nagapetyan, S. S.; Dolzhenko, Y. I.; Arakelova, E. R.; Koshkin, V. M.; Struchkov, Y. T.; Shklover, V. E. *Russ. J. Inorg. Chem.* **1988**, *33*, 1614.

(27) Takahashi, J. Master Thesis, Tohoku University, 1989.

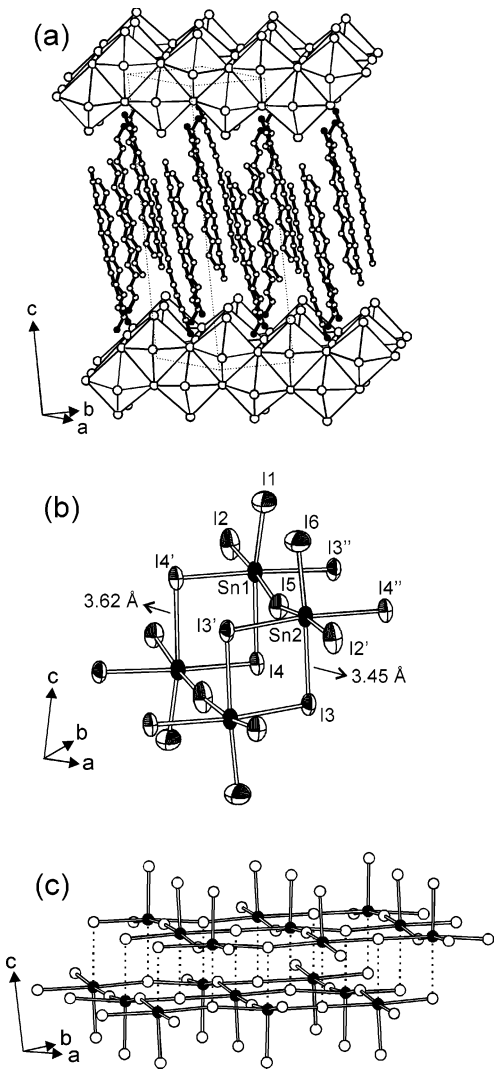

Figure 2. Crystal structure of **1**. (a) The overall lamellar structure with the SnI_3^- layers shown in a polyhedral representation and the C and N atoms of the dodecylammonium layer shown as unfilled (○) and black circles (●), respectively. (b) Thermal ellipsoids (50% probability) and atom labeling for a fragment of the SnI_3^- layer. Atoms related by an inversion center are differentiated by an apostrophe (e.g., I3 and I3′). The two longest Sn−I bond (secondary bond) distances are marked. (c) The SnI_3^- layer with the secondary Sn−I bonds shown as dotted lines to highlight the two subsidiary sheets that are based on square pyramidal SnI_5 units sharing the basal vertices. Sn: black sphere (●); I: unfilled sphere (○).

provided by the unshared iodine atom (bond lengths, Sn1−I1, 2.90 Å; Sn2−I6, 2.93 Å), and opposite (trans) to it, one finds the longest bond (bond lengths, Sn1−I4, 3.62 Å; Sn2−I3, 3.45 Å). Thus, along the direction of I1−Sn1−I4 (or I6−Sn2−I3), the strongest distortion occurs. (2) The second strongest distortion is found with the iodine atoms shared by two octahedra, namely, along the direction I2−Sn1−I5 (or I5−Sn2−I2′), with the following bond lengths: Sn1−I2, 3.09 Å; Sn1−I5, 3.23 Å (or Sn2−I5, 3.07 Å; Sn2−I2′, 3.24 Å). (3) The least distortion occurs along I3″-Sn1−I4′ (or I4″-Sn2−I3′), where both iodine atoms belong to three adjacent SnI_6 octahedra. Here, the two alternating bonds are only slightly different: Sn1−I3″, 3.15 Å; Sn1−I4′, 3.19 Å (or Sn2−I4″, 3.166 Å; Sn2−I3′, 3.174 Å). Elongated bonds such as Sn1−I4 and Sn2−I3 can be considered secondary bonds (cf. sum of covalent, ionic, and van der Waals radii of Sn and I are 2.68, 3.16, and 4.15 Å, respectively[28]) and are generally indicative of the stereochemical activity of the $5s^2$ lone pair on the Sn(II) ion.[28] The strong distortion of the SnI_6 octahedra in the layers of **1** contrasts with what is usually observed in primary ammonium-templated SnI_4^{2-} or PbI_4^{2-} perovskite sheets, where the lone pair activity tends to be largely suppressed, with rather small distortion of the SnI_6 and PbI_6 octahedra. For comparison with **1**, the Sn−I bond lengths in $[CH_3(CH_2)_{11}NH_3]_2SnI_4$ only vary from 3.13 to 3.15 Å.

The distortions of the SnI_6 octahedra point to a second way of visualizing the MoO_3-type slab in **1**. If the longest Sn−I bond is excluded, the bonding geometry around the Sn(II) atom becomes similar to a square pyramid. As is shown in Figure 2c, such square pyramids share the basal vertices and constitute two subsidiary sheets within each SnI_3^- layer. The two subsidiary sheets adhere to each other by means of the secondary Sn−I bonds and in so doing build up the entire SnI_3^- layer. Within the subsidiary sheet, the four Sn−I−Sn bond angles (e.g., Sn1−I5−Sn2 in Figure 2b) are 174.6°, 171.6°, 176.5°, and 163.1° for the I2, I3, I4, and I5 atoms, respectively. Such values are larger than most Sn−I−Sn bond angles observed in various SnI_4^{2-}-based perovskites (cf. the Sn−I−Sn angle in $[CH_3(CH_2)_{11}NH_3]_2SnI_4$ is 155.7°).[17,20] Note that for the well-studied SnI_4^{2-} systems, larger Sn−I−Sn bond angles have been found to be generally associated with smaller band gaps of the hybrid semiconductors. Further study on structural analogues of **1** using different organic cations will help verify if similar correlation exists in this more complex type of network.

To conclude, compound **1**, with its MoO_3-type Sn(II)−I framework, represents a step beyond the familiar domain of perovkites in our search for solution-processable hybrid semiconductors. The thicker MoO_3-type layer in **1** apparently contributes to the distinct narrowing of the electronic band gap, with regard to the perovksite counterpart $[CH_3(CH_2)_{11}NH_3]_2SnI_4$. The increased dimensionality of the Sn−I framework in **1** may also provide more extensive pathways for the migration of charge carriers, thereby improving the semiconductive properties such as charge carrier mobilities. We also envision that other hybrid systems of formula $(RNH_3)MX_3$ (M = divalent metal; X = halogen; R = organic moiety) may adopt this structural type and be accessible either through solution- or melt-based techniques or as an intermediate in the thermal decomposition of $(RNH_3)_2MX_4$.[29]

Supporting Information Available: Full crystallographic data in CIF format for **1** and its perovskite analogue $[CH_3(CH_2)_{11}NH_3]_2SnI_4$. Table of Sn−I bond distances and angles in **1**. Figure showing the overall crystal structure of $[CH_3(CH_2)_{11}NH_3]_2SnI_4$. X-ray diffraction patterns for powder and thin film samples of **1** and $[CH_3(CH_2)_{11}NH_3]_2SnI_4$. This material is available free of charge via the Internet at http://pubs.acs.org.

IC0347081

(28) Donaldson, J. D.; Grimes, S. M. *Rev. Silicon, Germanium, Tin Lead Compd.* **1984**, *8*, 1.
(29) Tello, M. J.; Bocanegra, E. H.; Arrandiaga, M. A.; Arend, H. *Thermochim. Acta* **1975**, *11*, 96.